Environmental Science Nano

Dual roles of glutathione in silver nanoparticle detoxification and enhancement of nitrogen assimilation in soybean (*Glycine max* L.[Merrill])

Journal:	*Environmental Science: Nano*
Manuscript ID	EN-ART-02-2020-000147.R1
Article Type:	Paper

Environmental Significance

Silver nanoparticles (Ag NPs) have been widely applied in agriculture for the purpose of disease suppression. However, concerns over their environmental impacts, in particular on nitrogen fixation in legume plants, have drawn more attention in agricultural eco-systems. Micro-XRF spectra indicate that the majority of Ag in soybean root tissues was Ag-GSH. Thus, GSH was externally added into Ag NP-amended soil to investigate whether the presence of GSH could alleviate the Ag NP toxicity to soybean and elevate the N content simutaneously. Our results suggest that the addition of GSH not only significantly increased the fresh weight of Ag NP-treated soybean, but also elevated the total N content in both shoots and roots. Additionally, the amino acids profile further demonstrates that GSH could be utilized as a nitrogen source to detoxify Ag NPs and enhance plant growth. Our study shed light on developing nano-enabled technology for maintaining sustainable agriculture to minimize crop loss.

Dual roles of glutathione in silver nanoparticle detoxification and enhancement of nitrogen assimilation in soybean (*Glycine max* L. [Merrill])

Chuanxin Ma[1, 2], Hong Liu[3], Guangcai Chen[4], Qing Zhao[5], Huiyuan Guo[1], Rakesh Minocha[6], Stephanie Long[6], Yuanzhi Tang[7], Emily M. Saad[7], Roberto DeLaTorreRoche[2], Jason C. White[2], Baoshan Xing[1, *], and Om Parkash Dhankher[1, *]

[1]Stockbridge School of Agriculture, University of Massachusetts, Amherst, Massachusetts 01003, United States

[2]Department of Analytical Chemistry, The Connecticut Agricultural Experiment Station, New Haven, Connecticut 06504, United States

[3]College of Resources and Environmental Sciences, Fujian Agriculture and Forestry University, Fuzhou 350002, China

[4]Research Institute of Subtropical Forestry, Chinese Academy of Forestry, Fuyang, Zhejiang 311400, China

[5]Institute of Applied Ecology, Chinese Academy of Sciences, Shenyang 110016, China

[6]USDA Forest Service, NRS, 271 Mast Road, Durham, New Hampshire 03824, United States

[7]School of Earth and Atmospheric Sciences, Georgia Institute of Technology, Atlanta, Georgia 30332-0304, United States

Corresponding authors:

[*]Baoshan Xing: bx@umass.edu; Phone: 413-545-5212;

[*]Om Parkash Dhankher: parkash@umass.edu; Phone: 413-545-0062.

Abstract

Widespread use of silver nanoparticles (Ag NPs) as pesticides and fungicides in agriculture is a major environmental concern. In the present study, soybean (Glycine max L.) was grown in Ag NPs (0–62.5 mg/kg)–amended soil with or without the addition of glutathione (GSH). Ag NPs exerted severe phytotoxicity and caused the reduction of shoot and root biomass, total number of nodules or completely inhibited nodule formation at the doses above 31.25 mg/kg. Synchrotron–based techniques were applied to analyze Ag speciation in both the soil and soybean root tissues at harvest. The results indicate that the majority of Ag remained in the form of Ag NPs and that 23% was present as Ag2S in soil; in both root and nodule tissues, Ag–GSH was the main component (40.6-88%) other than Ag NPs (12-59.4%), highlighting the important role of GSH in alleviating the Ag NP-induced toxicity. The addition of 0.8 mM GSH not only significantly increased fresh biomass by 85% in the 62.5 mg/kg Ag NP treatment, but also decreased Ag accumulation by 24.8-27% in soybean tissues. Although the addition of 0.8 mM GSH reduced the nodule number and weight as compared to the control, the total nitrogen content in soybean co–treated with Ag NP and GSH was more than 5-fold higher than the Ag NP alone treatments, suggesting GSH may be utilized as a nitrogen source while simultaneously alleviating Ag NPs toxicity. The shoot and root contents of thiol-compounds (cysteine and gamma–glutamylcysteine) in the GSH treatments were several folds higher than the control and Ag NP alone treatments. Further, higher levels of essential amino acids, particularly alanine, glutamate, and glutamine which play important role in N assimilation in plants, in soybean across all the treatments further confirmed that GSH was utilized as a nitrogen source, resulting in enhanced soybean growth. Taken together, this study clearly demonstrated the negative impact of Ag NPs on soybean productivity and N fixation and highlights the protective role of GSH against Ag NP-induced toxicity. These findings have significant relevance for developing future strategies to minimize the crop loss in marginal or contaminated soils, subsequently enhancing global food security.

Keywords

Glycine max L., silver nanoparticles, glutathione, nitrogen fixation, amino acid profile

Introduction

Nanomaterials (NMs) have been synthesized and designed for a number of agricultural purposes, including the delivery of pesticides, fertilizers, and growth hormones, detecting plant pathogens and monitoring soil conditions.[1] Silver nanoparticles (Ag NPs) are one of the most commonly used metal–based NMs in agriculture and other industries. According to US Environmental Protection Agency (EPA), by 2018 there were 147 registered Ag–enabled pesticides in total, among which 77 contained Ag NPs.[2] As a consequence of direct application in agriculture (including processed sewage sludge), the released Ag NPs or the transformed Ag species could also end up in agricultural fields.[3] It is estimated that Ag concentrations in natural and sludge–treated soils could fall within a wide range of 0.1–133 mg/kg; however, the realistic concentrations were several orders of magnitude higher as compared to the predicted Ag concentration.[3, 4] Due to their specific properties, exposure to NMs may still pose potential risks in agricultural systems, although their efficacy at controlling crop diseases has become a promising technology to pursue.[5, 6] To date, the interactions between NMs and plants have been reviewed from a number of perspectives, including phytotoxicity, benefits, implications and applications in agriculture.[7, 8, 9] Sustainable management of natural resources is a primary aim in agriculture [10], and there is now a significant interest in nano–enabled approaches to meet that goal, including nanofertilizers and nanopesticides.[11, 12] Consequently, a thorough assessment of safety and risk is needed prior to widespread NP used in agriculture.

It is well known that legume plants are capable of establishing a symbiotic relationship with *Rhizobium* species through the formation of bacteria–filled nodules in the root system. Nitrogen fixing bacteria can trap atmospheric nitrogen (N_2) within these nodules and convert the gas to ammonia (NH_4^+), which is then bioavailable for plant uptake. The *Rhizobia*-legume symbiosis is one of the most important mutualistic relationships in agriculture.[13] However, a major concern is whether NPs introduction into agricultural system could disrupt nodule formation in leguminous

root systems, compromising the nitrogen cycle in soils and eventually leading to significant crop yield loss. Holden et al. (2018) commented that NMs might interfere with important plant–microbe symbiosis, and that the underlying mechanisms should be understood so as to ensure that NM applications are compatible with nitrogen fixing bacteria in agricultural applications.[14] Previous studies have demonstrated that at moderate to high concentrations, Ag NPs inhibited root length, decreased plant biomass, altered transpiration rate, and delayed plant development.[15, 16, 17, 18, 19, 20] In addition, NPs lowered nitrogen–fixation potential in soybean nodules, although no effect on nodules formation was evident upon exposure.[21] In order to compensate, additional N_2 fertilizers have to be applied in the field, which apart from being costly, could potentially cause additional environmental concerns such as N pollution of soil and ground water.

Glutathione (GSH) is an important biomolecule involved in plant defense against abiotic stresses (e.g. heavy metals, drought, and extreme temperature) and plays an essential role in the development of root nodules during symbiotic interactions in the soil.[22, 23, 24] It has been demonstrated GSH could serve as a ROS scavenger through the glutathione-ascorbate cycle in order to avoid the ROS–induced disruption of the nitrogen–fixation potential under abiotic stress conditions.[25] Clearly, GSH could participate in modulating nodule formation and the subsequent nitrogen fixation potential in the legume plants treated with NPs. Thus, we hypothesized that GSH could alleviate Ag NP–induced phytotoxicity and simultaneously modulate the N assimilation pathway in plants.

Soybean is one of the most widely cultivated crops, can fix 16.4 Tg N annually and represents 77% of the N fixed by the leguminous species.[26] Thus, in this work, soybean (William 82) was chosen as a model legume plant to investigate the dual roles of GSH in detoxifying Ag NP toxicity and enhancing N assimilation. Physiological parameters (biomass, photosynthetic efficiency, and total N content) and elemental analysis were measured to evaluate both Ag NP and GSH impacts on soybean growth. Synchrotron based X–ray fluorescence (μ–XRF) imaging

was applied to differentiate Ag species in soybean roots and nodules. In addition, the content of major thiol compounds in the GSH biosynthesis pathway and amino acids profile was measured to illustrate whether the external addition of GSH could counteract the Ag NP-induced phytotoxicity and biostimulate the seedling growth. Given that GSH significantly alleviates Ag nanotoxicity and enhances soybean growth, thiol compounds could become an important agricultural amendment for improving crop productivity under stress conditions.

Materials and Methods

Concentration selection of Ag NPs and GSH

The growth substrate, concentrations of Ag NPs and GSH were optimized prior to use. In this experiment, field soil was collected from the Agronomy Research Farm of the University of Massachusetts in South Deerfield and was mixed with 25% (*v/v*) vermiculite for the pot experiment. Detailed information (**Figure S1 and S2**) on substrate optimization is provided in **Text S1** in the supporting information (**SI**).

Soybean seeds (William 82 obtained from The United States Department of Agriculture) were sown in a plastic pot (4.5 inch in diameter by 4.5 inch in height) containing 250 g soil with water content at 40%. To determine the critical concentration of Ag NPs (particle size: 20 nm; US Research Nanomaterials, Inc.) that caused physiological damage to soybean, different concentrations of Ag NPs ranging from 3.9 to 62.5 mg/kg were prepared by thoroughly mixing different amounts of Ag NPs with the field soil. In addition, equivalent amounts of Ag in the form of silver nitrate ($AgNO_3$, Fisher Scientific) and bulk–sized Ag (particle size: 44 μm; Strem Chemicals) were used as the ionic Ag and bulk particle controls, respectively. The potted soil was stabilized for 24 h prior to use. Soybean seedlings were maintained under the greenhouse conditions (temperature: 25 °C; relative humidity: 74%; light intensity: 250 μmol $m^{-2}s^{-1}$; light period: 16/8, day/night) for 4–5 weeks. Fresh biomass and total number of nodules were used as endpoints to determine the selected concentrations of Ag NPs. In addition, photosynthetic

efficiency and total chlorophyll content across all treatments were measured. Detailed information for both methods is provided in **Text S2**.

For the concentration selection of GSH, different concentrations (5, 10 and 20 mmol L^{-1}) of GSH solution (L–Glutathione reduced, Sigma–Aldrich) were prepared in 50 mL deionized H_2O. A volume of 10 mL of the prepared GSH solution was applied to each pot once per week over 4 weeks. Thus, the final concentration in each GSH treatment was 0.8, 1.6 and 3.2 mmol per kg of soil, respectively, corresponding to 4–time additions of 10 mL of 5, 10 and 20 mmol per liter of GSH solution. Fresh biomass and the total number of nodules were used to determine the selected concentrations.

Pot experiment

Based on the above experiments, 31.2 and 62.5 mg/kg Ag NPs and 0.8 mM GSH were used in the pot experiment. Soybean seeds were germinated and grown in either Ag NPs alone treatments or with co–exposure to GSH under identical greenhouse conditions. Seedlings grown in the field soil alone or 0.8 mM GSH–amended soil were established as controls. Six biological replicates were applied in each treatment. At harvest, the plant tissues were either oven–dried or stored at –80 °C until further analysis.

Determination of Ag and nutrient content in soybean tissues

Soybean tissues (shoots, roots, and nodules) were oven dried and then ground into fine powders. Approximately 50 mg of sample were transferred into a digestion tube containing 3 mL of concentrated HNO_3 and the samples were digested at 105 °C for 40 min. Then, 500 µL of H_2O_2 were added into each tube for another 20 min of heating at 105 °C to complete the digestion. The digest was diluted to 50 mL with deionized prior to analyze. Inductively coupled plasma mass spectroscopy (ICP-MS, Agilent 7700x, Santa Clara, CA) was used to determine the Ag concentration. The concentration of both macro– (K, Mg, P, Ca, S) and micronutrients

(Cu, Zn, Mn, Fe) were determined by inductively coupled plasma optical emission spectrometry (ICP–OES, iCAP6000 Series, Thermo Scientific, Waltham, MA). A four-point calibration curve of Ag and other elements was prepared using standard reference materials (SPEX CertiPrep, Metuchen, NJ). To ensure the quality of the measurement, yttrium (Y) was used as an internal standard and a sample of known concentration was measured every 12 samples.

Bulk X–ray absorption spectroscopy (XAS)

Ag K–edge bulk XAS analysis of the soils after soybean growth in the presence of 31.25 mg/kg Ag NPs was conducted on Beamline 5-BM-D at Advanced Photo Source (APS; Argonne National Laboratory, Lemont, IL). Ag foils were used as energy calibration. Soil samples collected at soybean harvest and plant fresh tissues, which were freeze–dried and ground into fine powders, were packed into a Teflon sample holder and covered with Kapton tapes. X–ray absorption near edge structure (XANES) data were collected in fluorescence mode using a vortex detector. XAS data were also collected on a range of reference compounds, including Ag_2S, Ag_3PO_4, AgCl, $AgNO_3$, Ag–citrate, Ag NPs, citrate–coated Ag NPs and Ag–GSH complex. All silver compounds were purchased from Sigma–Aldrich. Ag NPs and citrated–coated Ag NPs were obtained from US Research Nanomaterials, Inc. and nanoComposix, Inc., respectively. Ag–GSH was synthesized as described by Larue et al.[27] XAS data were processed and analyzed using the software Ifeffit.[28, 29] Multiple scans were energy calibrated and averaged for further analysis. Principal component analysis (PCA) was conducted to determine the number of components needed to obtain reasonable fits. Using the corresponding reference compound spectral library, target transformation was examined to determine appropriate candidate compounds. Linear combination fitting (LCF) was conducted on XANES data at –30 to 130 eV to elucidate the relative contribution of each component. R-factor was used to determine the goodness of fit.

Micro X–ray fluorescence (μ–XRF) imaging and μ–XAS analysis

Synchrotron μ–XRF imaging and μ–XAS analysis were conducted on the soybean biomass samples at Beamline 20–ID–B at APS. Both whole and cross sections of soybean nodules, roots, and leaves were analyzed. Cross sections of the plant tissues were obtained by embedding the samples in Tissue-Tek O.C.T. compounds, followed by cryo-sectioning to 100 μm using a cryostat (TEP CryoStar NX70, ThermoFisher Scientific, Waltham, MA, USA). The produced thin sections were mounted onto glass slides. All samples were stored at –80 °C and transported to the beamline on dry ice. Whole root, nodule, or leaf samples were directly mounted on Kapton tape. At the beamline, sample–loaded glass slides or Kapton tapes were mounted on a sample stage cooled down by a Linkam cryostage to liquid nitrogen temperature. Samples were raster scanned under the beam at an energy of 26 KeV and step size of $2 \times 2\ \mu m^2$. At selected hot spots, Ag K–edge μ–XANES spectra were collected to reveal the structural information. Processing of image data used the software ImageJ. LCF analysis of the μ–XANES data used the same procedure as the bulk XAS data analysis.

Total nitrogen analysis

Soybean tissues (leaf, root and nodule) were freeze-dried using a Lyophilizer (FREEZONE 4.5, LABCONCO, Kansas City, MO, USA) and were then ground into fine powders for Kjeldahl digestion. Briefly, 0.2 g of tissue and 1.625 g mixture of potassium sulfate and cupric sulfate were added into a Kjeldahl flask. A volume of 3.5 mL H_2SO_4 was added into each flask and heated at 160 °C till the solution became clear. Then, all the digests were heated at 390 °C until green color was observed. All digests were cooled down in a hood and were diluted with 46.5 mL deionized H_2O. The total nitrogen concentration was measured using a QC8500 analyzer (Lachat Instruments, Loveland, CO, USA).

Inhibition curve and dehydrogenase activity of Ag NP treated *Bradyrhizobium*

It was previously reported that the abundance of *Bradyrhizobium* in the collected soil was greater than that of *Frankia* and *Rhizobium*.[30] Thus, *Bradyrhizobium japonicum* (USDA 110) was used to test the effects of Ag NPs on rhizobium growth in HEPES–MES (HM) medium with or without the addition of GSH. The total number of colony-forming unit (CFU) was counted at Day 1, 2, 3, 5 and 7 across all the treatments and dehydrogenase activity of *Bradyhizobium* was also measured at Day 7.[31] Details are provided in **Text S3 and Table S1**.

Analysis of thiol compounds and amino acids

For thiol compounds measurement, approximately 200 mg of fresh soybean tissues were extracted in 1.5 mL of buffer containing 6.3 mM diethylenetrianmine pentacetic acid, DTPA, mixed with 0.1% trifluoroacetic acid (TFA). The content of cysteine, γ–glutamylcysteine, and GSH in soybean tissues were measured as described in Minocha *et al.* (2008).[32] To determine the amino acid profile, 200 mg of fresh soybean tissue were extracted in 1 mL of 5% (*v/v*) ice cold perchloric acid and were stored at –20 °C. Procedures for sample preparation, HPLC setup, as well as sample separation were followed per Minocha & Long (2004)[33] with minor modifications described in Majumdar et al. (2018).[34]

Gene expression analysis by quantitative PCR

Soybean shoots or roots were homogenized in liquid nitrogen prior to RNA isolation. Procedures for total RNA isolation, cDNA synthesis, and gene expression using qPCR were described in Ma *et al*. (2013).[35] Detailed information is provided in **Text S4 and Table S2**. Relative quantities ($2^{-\Delta\Delta Ct}$ method) were used to calculate the transcription level of each gene.

Statistical analysis

For each assay, the means are averaged from 4–5 replicates and error bars correspond to standard error of mean. A one–way analysis of variance (One–way ANOVA) followed by Duncan multiple comparison test was used to determine statistical significance of each parameter among treatments. Values of each assay followed by different letters are significantly different at $p \leq 0.01$ or 0.05.

Results and Discussion

Part I: Ag NPs inhibited plant growth, nodule formation, and N_2 fixation

Physiological responses of soybean upon Ag NP exposure

Physiological results suggest that size-effect of Ag particles is a primary factor that determines Ag NP-induced abiotic stresses to soybean seedlings in terms of fresh biomass, photosynthesis efficiency, nodule formation and total N content (**Figure S3-S5**). Detailed information is provided in **Text S5**. It is noted that the equivalent amounts of Ag in the form of Ag ions and bulk-sized Ag particles had no impact on either fresh weight or nodule formation. Aligning with our results, exposure to a mixture of metal–based NPs (Ag, ZnO and TiO_2) decreased the total number of nodules in alfalfa more than 13–fold as compared to the control and bulk-sized particle treated one.[36] Wang *et al*. (2018) also reported that carbonaceous NMs reduced the total plant nitrogen fixation potential by over 90%.[37]

Ag NP biotransformation in soil and soybean roots

Synchrotron-based technique was used to differentiate the Ag species in Ag NP amended soil as well as soybean tissues. XAS analysis of the soil-plant system suggests transformation of Ag NPs into other Ag species. Spectra of the reference compounds used for LCF analysis are shown in **Figure S6**. Bulk XAS spectra of Ag NP–amended soil shows that more than 75% of Ag species were still in the form of Ag NPs, but the presence of 23% Ag_2S indicates that

sulfidation had occurred (**Figure 1A**). These findings are consistent with other studies evaluating Ag NP transformation in soil and biological systems.[38]

Synchrotron μ–XRF images show the Ag distribution in cross–sections of nodule, root, and the whole root samples (**Figure 1B, D, and G**). Subsequent XANES spectra and LCF analysis suggest that Ag–GSH is the primary Ag species in Ag NP–treated soybean roots and nodules. For example, approximately one third of Ag in the nodule was Ag–GSH (**Figure 1C**); 40.6–88% Ag–GSH was found in the cross–section of root (**Figure 1E–F**) and in the whole root, only Ag–GSH was present in the analyzed regions (**Figure 1H–I**). Other XANES spectra in Ag NP–treated soybean root tissues also indicate that the main Ag species in Ag NP–treated roots were as Ag–thiol compounds or Ag_2S in **Figure S7.** The Ag content in plant leaves was below the detection limit for both bulk XAS and XRF. Similarly, the main Ag species in foliar Ag NP–treated lettuce was either Ag NPs themselves or Ag–GSH, indicating that Ag NPs could penetrate the stomata or cuticle and accumulate in leaves.[27] Importantly, Ag–GSH was a significant component resulting from the interaction of Ag NPs with the plant, likely as a detoxification mechanism.[39]

Part II: GSH significantly alleviates Ag nanotoxicity in soybean

Physiological response

In order to investigate the role of GSH in alleviating Ag NP-induced toxicity, GSH was exogenously added into Ag NP-amended soil. Detailed information for the GSH optimization is provided in **Text S6** (**Figure S8 and S9**). Exposure to 62.5 mg/kg Ag NPs severely inhibited soybean growth and decreased the fresh weight by 28.8% (**Figure 2A–C**). However, the addition of 0.8 mM GSH significantly increased the total fresh weight of 62.5 mg/kg Ag NP–treated soybean to the GSH control level; this corresponded to an approximately 85.3% increase in the total fresh weight of co–treated soybean when comparing to the 62.5 mg/kg Ag

NP treatment alone (**Figure 2C**), indicating that GSH could potentially alleviate the Ag NP–induced phytotoxicity and be used as a nitrogen source for plant growth. It is worth noting that the presence of 0.8 mM GSH significantly lowered the total number and fresh weight of nodules as compared to the non–GSH control (**Figure 2D and E**). GSH is a tri–peptide made of glutamate (Glu), cysteine (Cys) and glycine (Gly), and is the source of glutamate (Glu), the first amino acids synthesized from the N assimilation pathway. The exogenously applied GSH might be used by soybean seedling as a nitrogen source for plant growth.

Ag and essential nutrients contents

In the Ag NP alone treatments, the root Ag content increased in a dose–dependent manner; interestingly, the addition of GSH yielded a decreasing trend of Ag content in roots as compared to the corresponding Ag NP alone treatment (**Figure 3A**). The Ag content in soybean shoots is negligible across all the treatments, and the addition of GSH in nodules treated with 31.2 mg/kg Ag NPs did not significantly alter the Ag accumulation as compared to the GSH control or the corresponding Ag NP alone treatment. Regarding essential nutrients, both Ag NPs and GSH significantly altered the content of most macro– and micronutrients in the soybean tissues (**Figure 3B–H**). The addition of GSH increased the Mg content in 31.2 mg/kg Ag NP–treated shoots by 25.4% over the corresponding Ag NP alone treatment. Similarly, 68.9% and 110.7% increases in the root Mg content in the co-exposure treatment were evident as compared to the 31.2 and 62.5 mg/kg Ag NP alone treatment, respectively (**Figure 3B**). Similar increase was also found for other macronutrients, such as P, Ca, and K in soybean tissues co–exposed to Ag NPs and GSH (**Figure 3C–E**). Notably, GSH had an even greater impact on increasing the micronutrient content in soybean (**Figure 3F–H**). For example, the Cu content in the co–treated tissues was more than 2–fold that of the Ag alone treatment (**Figure 3F**). A similar trend was also evident in Mn and Zn accumulation in soybean upon external addition of GSH (**Figure**

3G–H). The up-regulation of genes encoding divalent metal transporter (*DMT*) in the Ag NP treatment with the GSH addition might explain the enhanced micronutrient uptake by soybean (**Figure S10A**). Details for other nutrients, including Na, S, and Fe are presented in **Figure S11**. Thus, the elevation in essential nutrient contents in soybean likely contributed greatly to the enhancement of soybean growth and potentially counteracted some of the Ag NP–induced phytotoxicity.

Nitrogen content

The exogenous application of GSH increased the N content in shoots and roots in a dose–dependent manner (**Figure 4A**). Exposure to 62.5 mg/kg Ag NPs decreased the shoot N content by approximately 50% as compared to the control; however, the addition of GSH significantly increased the shoot N content by more than 5–fold as compared to the Ag NP treatment alone (**Figure 4B**). Conversely, GSH decreased the nodule N content (**Figure 4C**), which is consistent with decreases in the number and fresh weight of nodules as affected by the GSH addition (**Figure 2D–E**). High dose of Ag NPs exposure decreased the N content by approximately 40% in the root system, whereas the addition of GSH significantly increased the N content as compared to the corresponding Ag NP alone treatment (**Figure 4D**). It appears that in addition to alleviating the negative effects of Ag NPs on nitrogen assimilation and overall plant health, the exogenous application of GSH could also be utilized as a nitrogen source.

An *In vitro* assay assessing the interaction between *Bradyrhizobium* and Ag NPs, GSH, and Ag NPs+GSH was conducted and the total number of colony-forming unit (CFU) in the treatments with Ag NPs and GSH was higher as compared to the corresponding Ag NP alone treatments (**Figure S12A**). However, in comparison with the control, the addition of 0.8 mM GSH significantly decreased the total number of CFU; also, dehydrogenase (DHA) activity further confirmed this result (**Figure S12B**). Importantly, significant downregulation of the gene

encoding nodule signaling (*PLCX*) was found in soybean roots across all the treatments (**Figure S10B**), except the control, suggesting GSH and Ag NPs could both alter the nodulation and total number of nodules. However, both analytes had the completely opposite impact on soybean growth. Asadishad *et al*. (2018) reported that in comparison with ZnO and CuO NPs, Ag NPs significantly inhibited the soil enzymes at 100 mg/kg and subsequently changed the soil microbial community composition.[40] Several studies demonstrated that both carbonaceous NMs and metal–based NPs could significantly alter the composition and function of rhizosphere microbial community.[36, 41, 42] Moreover, significant downregulation of genes encoding nodule–specific glycine–rich protein in alfalfa upon exposure to a mixture of metal–based NMs was reported.[43] Overall, NMs may interrupt the signaling between legumes and *rhizobium*, lower the abundance of *rhizobium* in the rhizosphere, and eventually interfere the N fixation in agriculture.

Thiol compounds analysis

The content of thiol compounds involved in the GSH biosynthesis pathway was measured across all the treatments with or without the addition of GSH (**Figure 5**). The presence of Ag NPs at 31.2 and 62.5 mg/kg did not greatly affect the content of all three thiol compounds. However, the addition of 0.8 mM GSH elevated the thiol compounds content in soybean. For example, in the controls with GSH, there was no noticeable increase in the content of cysteine, γ–EC, and GSH in shoots relative to the GSH-free control (**Figure 5A–C**). Interestingly, in the presence of 31.2 mg/kg Ag NPs, the addition of 0.8 mM GSH resulted in 5 to 10–fold increase in the thiol compound content in the shoots. In comparison with the shoots, the root contents of the three thiol compounds were significantly increased in the GSH control relative to the GSH–free control (**Figure 5D–F**) and in the 31.2 mg/kg Ag NP treated roots, the addition of GSH also elevated the contents of these three thiol compounds. In the nodules, the content of cysteine and γ–EC in the GSH treatments with or without Ag NPs was approximately 2–fold of the control

or Ag NP alone treatment (**Figure 5G–H**). However, the external addition of GSH did not increase the nodule GSH content (**Figure 5I**). Similarly, the GSH content in shoots and roots co–treated with 62.5 mg/kg Ag NPs and external GSH was not significantly altered.

The GSH metabolic pathway is important in scavenging ROS generated by xenobiotics compounds.[44, 45] Because of thiol group (–SH), cysteine in GSH can effectively bind with Ag and lower its toxicity to plants.[20] Upon exposure to Ag NPs, transgenic *Crambe hispanica* subsp. *abyssinica* (Hochst. ex R.E.Fr.) Prina overexpressing bacterial γ-glutamylecysteine synthase (γ-ECS) exhibited strong tolerance to Ag NPs as compared to the wild type plants.[20] High levels of cysteine, γ–EC, and GSH in transgenic *Crambe* indicated the important role of the GSH metabolic pathway in defending terrestrial plants against abiotic stresses especially heavy metals. However, in the current work, the exogenous addition of GSH did not significantly increase the GSH level in soybean tissues across the most of treatments except shoots. We speculate that glutamate in GSH was being utilized as a nitrogen source and thereby increased N assimilation through further amino acid biosynthesis.

Amino acid profile

The external addition of different concentrations (0.8–3.2 mM) of GSH altered the amino acid profile in soybean (**Table S3–S4 and Text S7**). Three amino acids, alanine, glutamate and glutamine play important roles in N assimilation in plants. Not surprisingly, the addition of GSH significantly elevated the level of these three amino acids in both shoots and roots (**Figure 6**). For example, the addition of 0.8 mM GSH increased the shoot alanine and glutamate content by approximately 10– and 6–fold as compared to the GSH–free control, respectively (**Figure 6A and D**). Similar results were also evident in GSH treated roots co-exposed to Ag NPs (**Figure 6B and E**). Compared to the GSH–free control, the root glutamine content was increased by 50% in the treatment with 31.2 mg/kg Ag NPs and 0.8 mM GSH (**Figure 6H**). However, the shoot

glutamine content in the GSH treatment was not significantly increased due to the relatively large variance (**Figure 6G**). Regarding the amino acid content in the nodules, the impact of 0.8 mM GSH or Ag NPs on the nodule amino acids content was not as large or significant as in the shoots or roots (**Figure 6C, F, and I**).

The amino acid profile in the shoots, roots, and nodules across all the treatments is shown in **Figure 6J–L**. In addition to the above three amino acids, the content of histidine, methionine, lysine, leucine, and others in the shoots across all the GSH treatments was significantly elevated as compared to the GSH–free control or Ag NP alone treatment (**Figure 6J**). A similar trend was also evident in roots and nodules co–treated with Ag NPs and GSH (**Figure 6K and L**). Detailed information for the content of other essential amino acids in soybean is provided in **Table S5–7**. Cluster analysis (**Figure 6J and K**) suggests that the exogenous application of GSH significantly elevated the overall amino acids content in shoots and roots, especially in the 31.2 mg/kg Ag NP treatment. However, in nodules, the amino acids in the GSH alone treatment were separated from other three treatments; it is worth noting that the addition of GSH made the amino acids level similar to the control (**Figure 6L**). In a life cycle study, exposure to commercial Ag NPs not only lowered the total wheat grain weight, but also resulted in 13 and 11.8% decreases in the content of arginine and histidine, respectively.[46] Similar findings were also reported in wheat upon treatment with other metal oxide NPs (Cu, Zn and Ti).[47] Rui *et al*. (2017) reported that metal–based NPs could significantly alter the amino acid prolife in peanut grains and subsequently affect both crop quality and yield.[48] In the current study, a common trend is that the external addition of GSH significantly elevated the content of each amino acid. In addition, Ag NP concentrations might also affect the GSH utilization by soybean as the addition of GSH significantly lowered the Ag content in root tissues, indicating that partial GSH was used to interact with Ag NPs and subsequently lower the Ag uptake by soybean. Similarly, in the presence of GSH, the total root N in 62.5 mg/kg Ag NP treatment was

also notably lower as compared to the 31.2 mg/kg Ag NP treatment, suggesting that with increasing Ag NP concentrations, the portion of GSH being used as a nitrogen source was decreased. Overall, GSH could be utilized as a nitrogen source by soybean and alleviate the Ag NP-toxicity simultaneously.

At the molecular level, genes encoding alanine aminotransferase (*ALAAT2* and *ALAAT3*) were downregulated in the Ag NPs alone treatment (**Figure S13**); in addition, the presence of Ag NPs decreased the relative expression of nitrite reductase (*NIR*) in soybean roots (**Figure S14**). Notably, the addition of GSH returned the levels of these genes to the control or even up–regulated them. For example, the relative expression of *NIR* and nitrate reductase (*NAR*) in shoots in the treatment with GSH was more than 2–fold greater than the corresponding GSH–free control (**Figure S14**), suggesting that GSH indeed participated in the N assimilation pathway and as such, defended soybean against Ag NP–induced stress. Taken together, the findings demonstrate that the external addition of GSH can facilitate the N assimilation pathway and up–regulate the further amino acid biosynthesis, subsequently enhancing plant growth and activating plant defense systems to counteract the Ag NP–induced phytotoxicity.

Conclusion

Exposure to Ag NPs could significantly alter the nodule formation and subsequently affect the N_2 fixation in soybean. Ag speciation in soybean tissues indicated that Ag–GSH was the main component other than Ag NPs, highlighting the important role of GSH in alleviating the Ag NP–induced toxicity. The exogenous addition of GSH to soybean demonstrated that GSH could reduce the Ag–induced toxicity to soybean and significantly enhance plant growth. It is noted that the GSH addition increased the N content in soybean tissues several–fold higher than the Ag NP alone treatments, suggesting that GSH might be utilized as a nitrogen source. Amino acid profile, particularly the levels of alanine, glutamate, and glutamine in N assimilation,

further confirmed GSH was utilized as a nitrogen source, resulting in enhanced soybean growth. Our overall findings suggest that engineered NPs could compromise the N_2 assimilation in legume crops via disrupting the nodule formation; developing strategies for designing crops that could synthesize high level of GSH itself or improving the manufacturing techniques that could lower the cost of thiol compounds will be useful to minimize crop loss, subsequently enhancing global food security and safety.

Supporting information

There are 7 texts, 27 figures and 7 tables in the supplementary file.

Acknowledgements

This research was supported by USDA–AFRI (2011–67006–30181) and USDA–NIFA Hatch program (MAS 00549, MAS 00401, CONH 00147). Y. Tang acknowledges the funding support from Georgia Water Resource Institute. We appreciate the support from beamline scientists Drs. Mali Balasubramanian and Chengjun Sun at APS Beamline 20–ID–B and Dr. Qing Ma at APS Beamline 5–BM–D. Portions of this research were conducted at the Advanced Photon Source (APS). Use of the Advanced Photon Source was supported by the U.S. Department of Energy, Office of Science and Office of Basic Energy Sciences. H. Liu acknowledges FAFU Technology and Innovation Project (KFA17149A).

Author Contributions

C.M., O.P.D. and B.X. designed the experiment. C.M. and H.L. conducted the experiment. G.C., H.G. and Q.Z helped with plant maintenance in the greenhouse and photosynthesis measurement. R.M. and S.L. measured the amino acid content in soybean tissues. Y.T. and E.S. analyzed the micro-XRF spectra. R.D. and J.C.W. measured the Ag and other nutrient

content in soybean tissues. C.M. wrote the manuscript. C.M., J.C.W., O.P.D. and B.X. revised the manuscript. All the authors approved the final manuscript.

Conflict of Interest

The authors declare no conflict of interest.

References

1. Parisi, C.; Vigani, M.; Cerezo, E. R. *Proceedings of a Workshop on" Nanotechnology for the agricultural sector: from research to the field"*; Institute for Prospective and Technological Studies, Joint Research Centre: 2014.
2. Wang, P.; Lombi, E.; Menzies, N. W.; Zhao, F.-J.; Kopittke, P. M., Engineered silver nanoparticles in terrestrial environments: a meta-analysis shows that the overall environmental risk is small. *Environmental Science: Nano* **2018,** *5* (11), 2531-2544.
3. Sun, T. Y.; Bornhöft, N. A.; Hungerbühler, K.; Nowack, B., Dynamic probabilistic modeling of environmental emissions of engineered nanomaterials. *Environmental science & technology* **2016,** *50* (9), 4701-4711.
4. Blaser, S. A.; Scheringer, M.; MacLeod, M.; Hungerbühler, K., Estimation of cumulative aquatic exposure and risk due to silver: contribution of nano-functionalized plastics and textiles. *Science of the total environment* **2008,** *390* (2-3), 396-409.
5. Borgatta, J.; Ma, C.; Hudson-Smith, N.; Elmer, W.; Plaza Pérez, C. D.; De La Torre-Roche, R.; Zuverza-Mena, N.; Haynes, C. L.; White, J. C.; Hamers, R. J., Copper Based Nanomaterials Suppress Root Fungal Disease in Watermelon (Citrullus lanatus): Role of Particle Morphology, Composition and Dissolution Behavior. *ACS Sustainable Chemistry & Engineering* **2018,** *6* (11), 14847-14856.
6. Ma, C.; Borgatta, J.; De La Torre Roche, R.; Zuverza-Mena, N.; White, J. C.; Hamers, R. J.; Elmer, W., Time-dependent transcriptional response of tomato (Solanum lycopersicum L.) to Cu nanoparticle exposure upon infection with Fusarium oxysporum f. sp. lycopersici. *ACS Sustainable Chemistry & Engineering* **2019**.
7. Ma, C.; White, J. C.; Zhao, J.; Zhao, Q.; Xing, B. J. A. r. o. f. s.; technology, Uptake of engineered nanoparticles by food crops: characterization, mechanisms, and implications. **2018,** *9*, 129-153.
8. Iavicoli, I.; Leso, V.; Beezhold, D. H.; Shvedova, A. A., Nanotechnology in agriculture: Opportunities, toxicological implications, and occupational risks. *Toxicology and applied pharmacology* **2017,** *329*, 96-111.
9. Rai, P. K.; Kumar, V.; Lee, S.; Raza, N.; Kim, K.-H.; Ok, Y. S.; Tsang, D. C., Nanoparticle-plant interaction: Implications in energy, environment, and agriculture. *Environment international* **2018,** *119*, 1-19.
10. Bourguignon, F.; Bénassy-Quéré, A.; Dercon, S.; Estache, A.; Gunning, J.; Kanbur, R.; Klasen, S.; Maxwell, S.; Platteau, J.; Spadaro, A., Millennium Development Goals at Midpoint: Where Do We Stand and Where Do We Need to Go? European Report on Development. 2008.

11. Prasad, R.; Bhattacharyya, A.; Nguyen, Q. D., Nanotechnology in sustainable agriculture: recent developments, challenges, and perspectives. *Frontiers in microbiology* **2017,** *8*, 1014.
12. Kah, M.; Kookana, R. S.; Gogos, A.; Bucheli, T. D., A critical evaluation of nanopesticides and nanofertilizers against their conventional analogues. *Nature nanotechnology* **2018,** *13* (8), 677.
13. Masson-Boivin, C.; Giraud, E.; Perret, X.; Batut, J., Establishing nitrogen-fixing symbiosis with legumes: how many rhizobium recipes? *Trends in microbiology* **2009,** *17* (10), 458-466.
14. Holden, P. A.; Mortimer, M.; Wang, Y., Engineered Nanomaterials and Symbiotic Dinitrogen Fixation in Legumes. *Current Opinion in Environmental Science & Health* **2018**.
15. Asli, S.; Neumann, P. M., Colloidal suspensions of clay or titanium dioxide nanoparticles can inhibit leaf growth and transpiration via physical effects on root water transport. *Plant, cell & environment* **2009,** *32* (5), 577-584.
16. Kim, S.; Lee, S.; Lee, I., Alteration of Phytotoxicity and Oxidant Stress Potential by Metal Oxide Nanoparticles in Cucumis sativus. *Water Air Soil Pollut* **2012,** *223* (5), 2799-2806.
17. Lee, W.-M.; Kwak, J. I.; An, Y.-J., Effect of silver nanoparticles in crop plants Phaseolus radiatus and Sorghum bicolor: Media effect on phytotoxicity. *Chemosphere* **2012,** *86* (5), 491-499.
18. Feng, Y.; Cui, X.; He, S.; Dong, G.; Chen, M.; Wang, J.; Lin, X., The role of metal nanoparticles in influencing arbuscular mycorrhizal fungi effects on plant growth. *Environmental science & technology* **2013,** *47* (16), 9496-9504.
19. Yoon, S.-J.; Kwak, J. I.; Lee, W.-M.; Holden, P. A.; An, Y.-J., Zinc oxide nanoparticles delay soybean development: A standard soil microcosm study. *Ecotoxicology and Environmental Safety* **2014,** *100* (0), 131-137.
20. Ma, C.; Chhikara, S.; Minocha, R.; Long, S.; Musante, C.; White, J. C.; Xing, B.; Dhankher, O. P., Reduced Silver Nanoparticle Phytotoxicity in Crambe abyssinica with Enhanced Glutathione Production by Overexpressing Bacterial γ-Glutamylcysteine Synthase. *Environmental science & technology* **2015,** *49* (16), 10117-10126.
21. Priester, J. H.; Ge, Y.; Mielke, R. E.; Horst, A. M.; Moritz, S. C.; Espinosa, K.; Gelb, J.; Walker, S. L.; Nisbet, R. M.; An, Y.-J.; Schimel, J. P.; Palmer, R. G.; Hernandez-Viezcas, J. A.; Zhao, L.; Gardea-Torresdey, J. L.; Holden, P. A., Soybean susceptibility to manufactured nanomaterials with evidence for food quality and soil fertility interruption. *Proceedings of the National Academy of Sciences* **2012,** *109* (37), E2451–E2456.
22. Yadav, S., Heavy metals toxicity in plants: an overview on the role of glutathione and phytochelatins in heavy metal stress tolerance of plants. *South African Journal of Botany* **2010,** *76* (2), 167-179.
23. Dixon, D. P.; Cummins, I.; Cole, D. J.; Edwards, R., Glutathione-mediated detoxification systems in plants. *Current opinion in plant biology* **1998,** *1* (3), 258-266.
24. Dalton, D. A.; Russell, S. A.; Hanus, F.; Pascoe, G. A.; Evans, H. J., Enzymatic reactions of ascorbate and glutathione that prevent peroxide damage in soybean root nodules. *Proceedings of the National Academy of Sciences* **1986,** *83* (11), 3811-3815.
25. Groten, K.; Vanacker, H.; Dutilleul, C.; Bastian, F.; Bernard, S.; Carzaniga, R.; Foyer, C. H., The roles of redox processes in pea nodule development and senescence. *Plant, Cell & Environment* **2005,** *28* (10), 1293-1304.
26. Herridge, D. F.; Peoples, M. B.; Boddey, R. M., Global inputs of biological nitrogen fixation in agricultural systems. *Plant and Soil* **2008,** *311* (1-2), 1-18.

27. Larue, C.; Castillo-Michel, H.; Sobanska, S.; Cécillon, L.; Bureau, S.; Barthès, V.; Ouerdane, L.; Carrière, M.; Sarret, G., Foliar exposure of the crop Lactuca sativa to silver nanoparticles: evidence for internalization and changes in Ag speciation. *Journal of hazardous materials* **2014,** *264*, 98-106.
28. Ravel, á.; Newville, M., ATHENA, ARTEMIS, HEPHAESTUS: data analysis for X-ray absorption spectroscopy using IFEFFIT. *Journal of synchrotron radiation* **2005,** *12* (4), 537-541.
29. Webb, S., SIXpack: a graphical user interface for XAS analysis using IFEFFIT. *Physica Scripta* **2005,** *2005* (T115), 1011.
30. COLE, E. J. ASSESSING KILN-PRODUCED HARDWOOD BIOCHAR FOR IMPROVING SOIL HEALTH IN A TEMPERATE CLIMATE AGRICULTURAL SOIL. Dissertation, 2015.
31. Burdock, T.; Brooks, M.; Ghaly, A., A dehydrogenase activity test for monitoring the growth of Streptomyces venezuelae in a nutrient rich medium. *Journal of Bioprocessing & Biotechniques* **2012,** *2011*.
32. Minocha, R.; Thangavel, P.; Dhankher, O. P.; Long, S., Separation and quantification of monothiols and phytochelatins from a wide variety of cell cultures and tissues of trees and other plants using high performance liquid chromatography. *Journal of Chromatography A* **2008,** *1207* (1), 72-83.
33. Minocha, R.; Long, S., Simultaneous separation and quantitation of amino acids and polyamines of forest tree tissues and cell cultures within a single high-performance liquid chromatography run using dansyl derivatization. *Journal of Chromatography A* **2004,** *1035* (1), 63-73.
34. Majumdar, R.; Lebar, M.; Mack, B.; Minocha, R.; Minocha, S.; Carter-Wientjes, C.; Sickler, C.; Rajasekaran, K.; Cary, J. W., The Aspergillus flavus Spermidine Synthase (spds) Gene, Is Required for Normal Development, Aflatoxin Production, and Pathogenesis During Infection of Maize Kernels. *Frontiers in plant science* **2018,** *9*, 317.
35. Hernandez-Viezcas, J. A.; Castillo-Michel, H.; Andrews, J. C.; Cotte, M.; Rico, C.; Peralta-Videa, J. R.; Ge, Y.; Priester, J. H.; Holden, P. A.; Gardea-Torresdey, J. L., In Situ Synchrotron X-ray Fluorescence Mapping and Speciation of CeO2 and ZnO Nanoparticles in Soil Cultivated Soybean (Glycine max). *ACS Nano* **2013,** *7* (2), 1415-1423.
36. Judy, J. D.; McNear Jr, D. H.; Chen, C.; Lewis, R. W.; Tsyusko, O. V.; Bertsch, P. M.; Rao, W.; Stegemeier, J.; Lowry, G. V.; McGrath, S. P., Nanomaterials in biosolids inhibit nodulation, shift microbial community composition, and result in increased metal uptake relative to bulk/dissolved metals. *Environmental science & technology* **2015,** *49* (14), 8751-8758.
37. Wang, Y.; Chang, C. H.; Ji, Z.; Bouchard, D. C.; Nisbet, R. M.; Schimel, J. P.; Gardea-Torresdey, J. L.; Holden, P. A., Agglomeration determines effects of carbonaceous nanomaterials on soybean nodulation, dinitrogen fixation potential, and growth in soil. *ACS nano* **2017,** *11* (6), 5753-5765.
38. Pradas del Real, A. E.; Castillo-Michel, H.; Kaegi, R.; Sinnet, B.; Magnin, V. r.; Findling, N.; Villanova, J.; Carrière, M.; Santaella, C.; Fernández-Martínez, A., Fate of Ag-NPs in sewage sludge after application on agricultural soils. *Environmental science & technology* **2016,** *50* (4), 1759-1768.
39. Cobbett, C. S., Phytochelatins and their roles in heavy metal detoxification. *Plant physiology* **2000,** *123* (3), 825-832.
40. Asadishad, B.; Chahal, S.; Akbari, A.; Cianciarelli, V.; Azodi, M.; Ghoshal, S.; Tufenkji, N., Amendment of agricultural soil with metal nanoparticles: effects on soil enzyme

activity and microbial community composition. *Environmental science & technology* **2018,** *52* (4), 1908-1918.
41. Ge, Y.; Shen, C.; Wang, Y.; Sun, Y.-Q.; Schimel, J. P.; Gardea-Torresdey, J. L.; Holden, P. A., Carbonaceous nanomaterials have higher effects on soybean rhizosphere prokaryotic communities during the reproductive growth phase than during vegetative growth. *Environmental science & technology* **2018,** *52* (11), 6636-6646.
42. Hao, Y.; Ma, C.; Zhang, Z.; Song, Y.; Cao, W.; Guo, J.; Zhou, G.; Rui, Y.; Liu, L.; Xing, B., Carbon nanomaterials alter plant physiology and soil bacterial community composition in a rice-soil-bacterial ecosystem. *Environmental pollution* **2018,** *232*, 123-136.
43. Chen, C.; Unrine, J. M.; Judy, J. D.; Lewis, R. W.; Guo, J.; McNear Jr, D. H.; Tsyusko, O. V., Toxicogenomic responses of the model legume Medicago truncatula to aged biosolids containing a mixture of nanomaterials (TiO2, Ag, and ZnO) from a pilot wastewater treatment plant. *Environmental science & technology* **2015,** *49* (14), 8759-8768.
44. Dalton, D. A.; Boniface, C.; Turner, Z.; Lindahl, A.; Kim, H. J.; Jelinek, L.; Govindarajulu, M.; Finger, R. E.; Taylor, C. G., Physiological roles of glutathione S-transferases in soybean root nodules. *Plant physiology* **2009,** *150* (1), 521-530.
45. Pauly, N.; Pucciariello, C.; Mandon, K.; Innocenti, G.; Jamet, A.; Baudouin, E.; Hérouart, D.; Frendo, P.; Puppo, A., Reactive oxygen and nitrogen species and glutathione: key players in the legume–Rhizobium symbiosis. *Journal of Experimental Botany* **2006,** *57* (8), 1769-1776.
46. Yang, J.; Jiang, F.; Ma, C.; Rui, Y.; Rui, M.; Adeel, M.; Cao, W.; Xing, B., Alteration of crop yield and quality of wheat upon exposure to silver nanoparticles in a life cycle study. *Journal of agricultural and food chemistry* **2018,** *66* (11), 2589-2597.
47. Wang, Y.; Jiang, F.; Ma, C.; Rui, Y.; Tsang, D. C.; Xing, B., Effect of metal oxide nanoparticles on amino acids in wheat grains (Triticum aestivum) in a life cycle study. *Journal of environmental management* **2019,** *241*, 319-327.
48. Rui, M.; Ma, C.; White, J. C.; Hao, Y.; Wang, Y.; Tang, X.; Yang, J.; Jiang, F.; Ali, A.; Rui, Y., Metal oxide nanoparticles alter peanut (Arachis hypogaea L.) physiological response and reduce nutritional quality: a life cycle study. *Environmental Science: Nano* **2018,** *5* (9), 2088-2102.

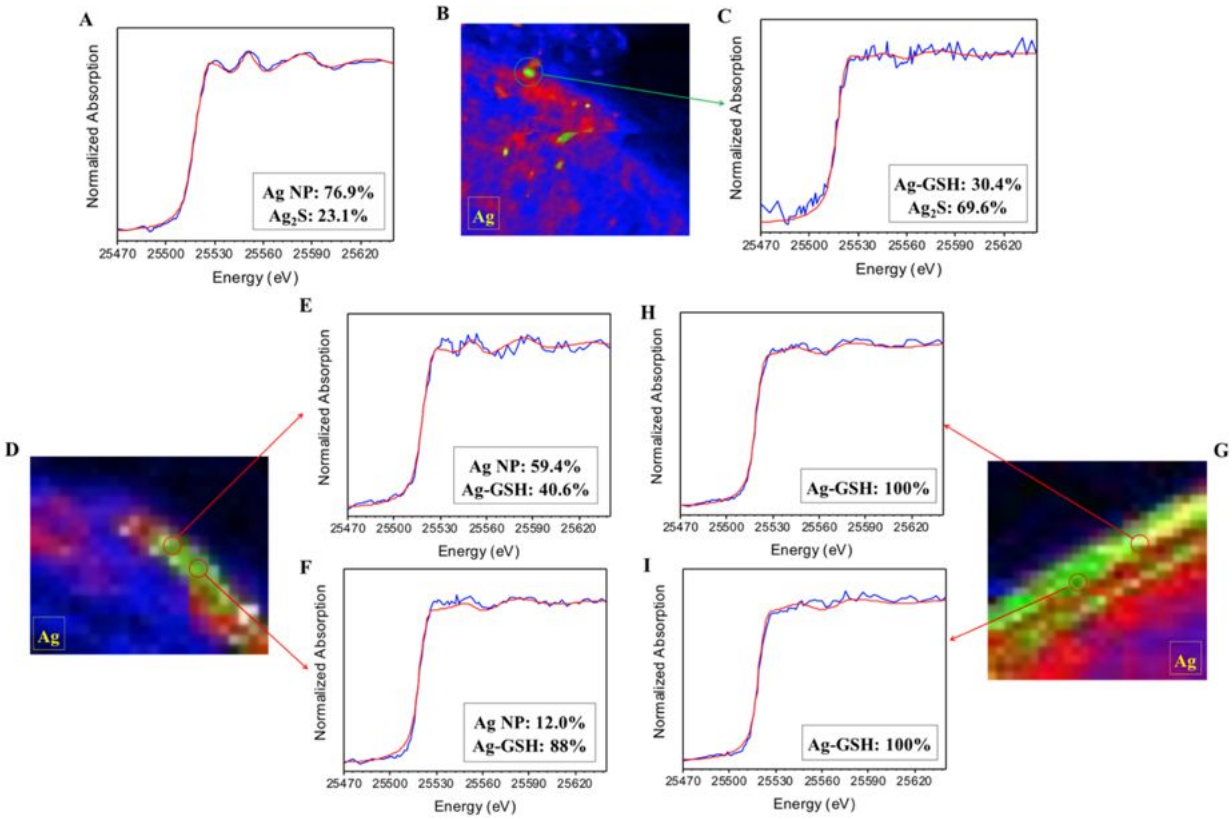

Figure 1. XAS analysis of soil, nodule, and root samples showing Ag transformation in the plant-soil system. **Figure A** is bulk Ag XAS spectra of soil sample after plant growth; **Figure B**, **D**, and **G** represents representative XRF images of nodule, root cross section, and whole root sample, respectively; **Figure C**, **E–F**, and **H–I** shows μ–XAS spectra (blue lines) of hot spots, as well as corresponding linear combination fitting results (red lines and insets) of nodule, root cross section, and whole root samples, respectively.

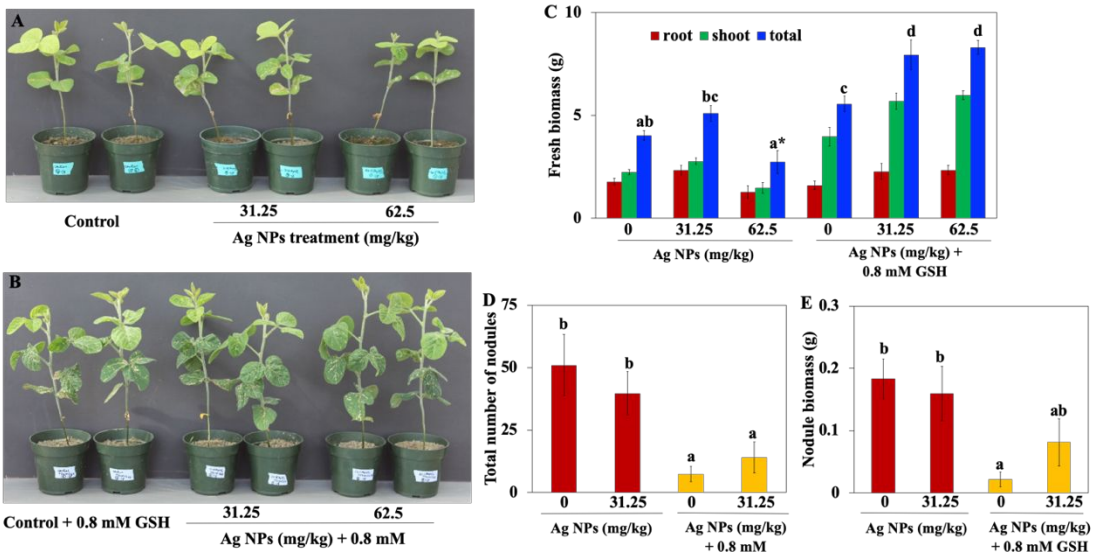

Figure 2. Physiological effects of GSH on the growth of Ag NPs treated soybean. Figure **A** and **B** represent phenotypic images of soybean treated with Ag NPs alone and Ag NPs + 0.8 mM GSH, respectively; Figure **C–E** represents fresh biomass, numbers of nodules, and nodule biomass, respectively. Error bars correspond to standard error of mean. Values of fresh biomass, nodule number or nodule weight followed by different letters are significantly different at $p < 0.05$. Single asterisk indicates that a significant difference ($p=0.0349$) between control and 62.5 mg/kg Ag NP treatment is evident by using a student t-test.

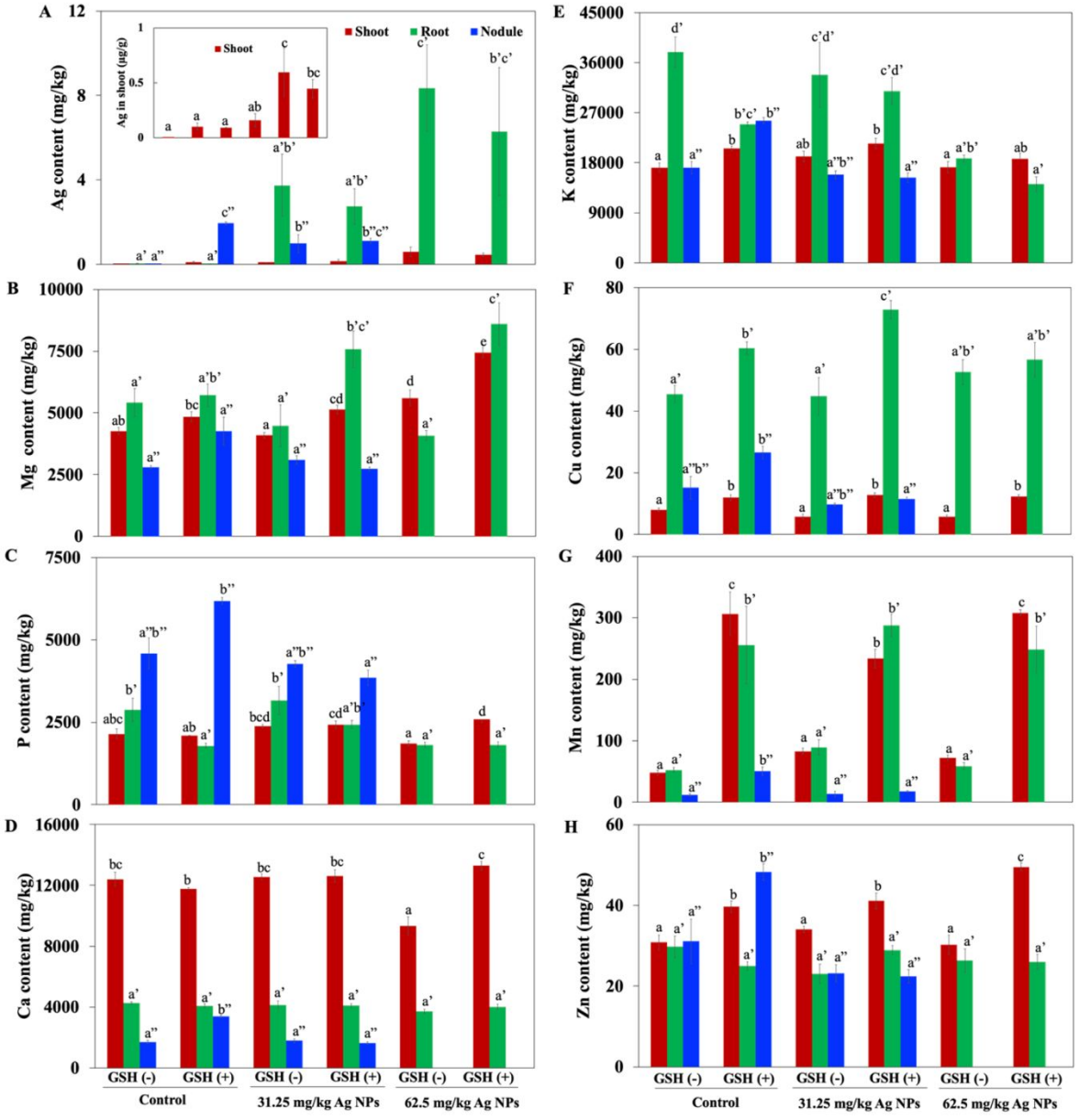

Figure 3. Ag and essential nutrient content in Ag NP treated soybean w/ or w/o the addition of 0.8 mM GSH. Figure **A** is the Ag content in soybean shoots, roots, and nodules; Figure **B**–**E** represents the content of macronutrients Mg, P, Ca, and K, respectively; Figure **F**–**H** shows the content of micronutrients Cu, Mn and Zn, respectively. Error bars correspond to standard error of mean. Values of each essential nutrient content in shoots followed by different letters are significantly different at $p < 0.05$; values of each essential nutrient content in roots followed by different letters with a single quotation mark are significantly different at $p < 0.05$; values of each essential nutrient content in nodules followed by different letters with double quotation marks are significantly different at $p < 0.05$.

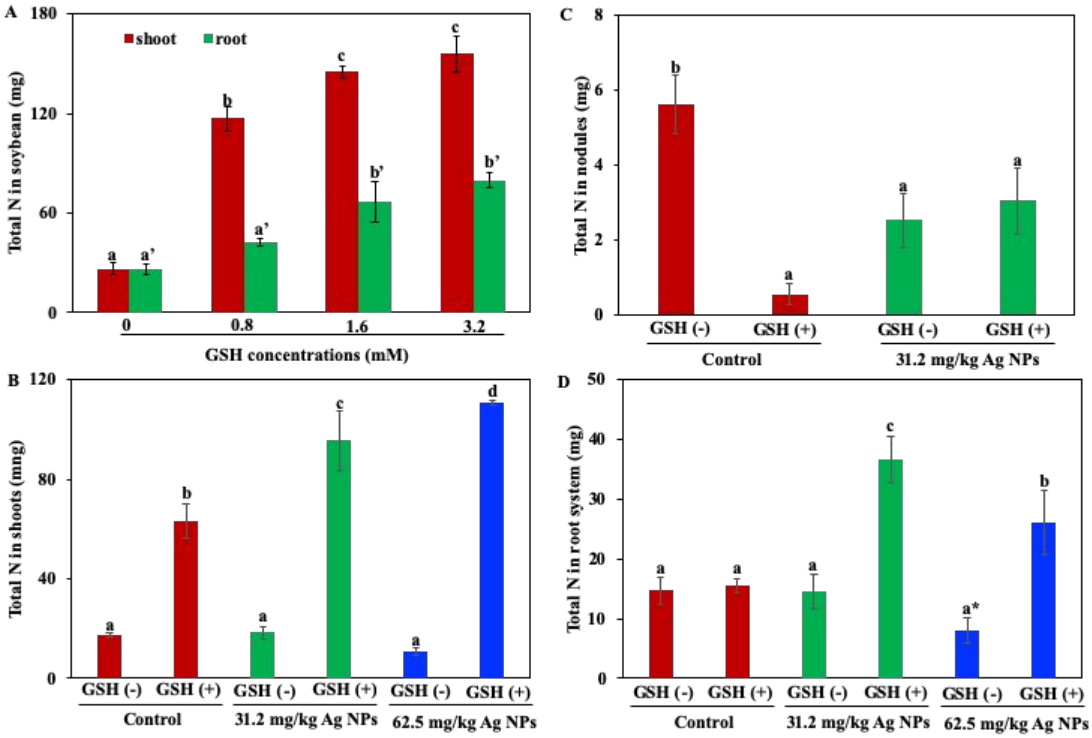

Figure 4. Total N in Ag NPs treated soybean w/ or w/o the addition of GSH. (**A**) effects of different concentrations of GSH on the total N level in soybean shoots and roots; (**B**) the total N level in shoots; (**C**) the total N level in nodules; (**D**) the total N level in the root system. Error bars correspond to standard error of mean. Values of total N in soybean tissues followed by different letters are significantly different at $p < 0.05$. In addition, in Figure 4A, different letters with single quotation mark indicate significantly different of total N in roots; single asterisk in Figure 4D indicates that a significant difference ($p=0.0228$) between control and 62.5 mg/kg Ag NP treatment is evident by using a student t-test.

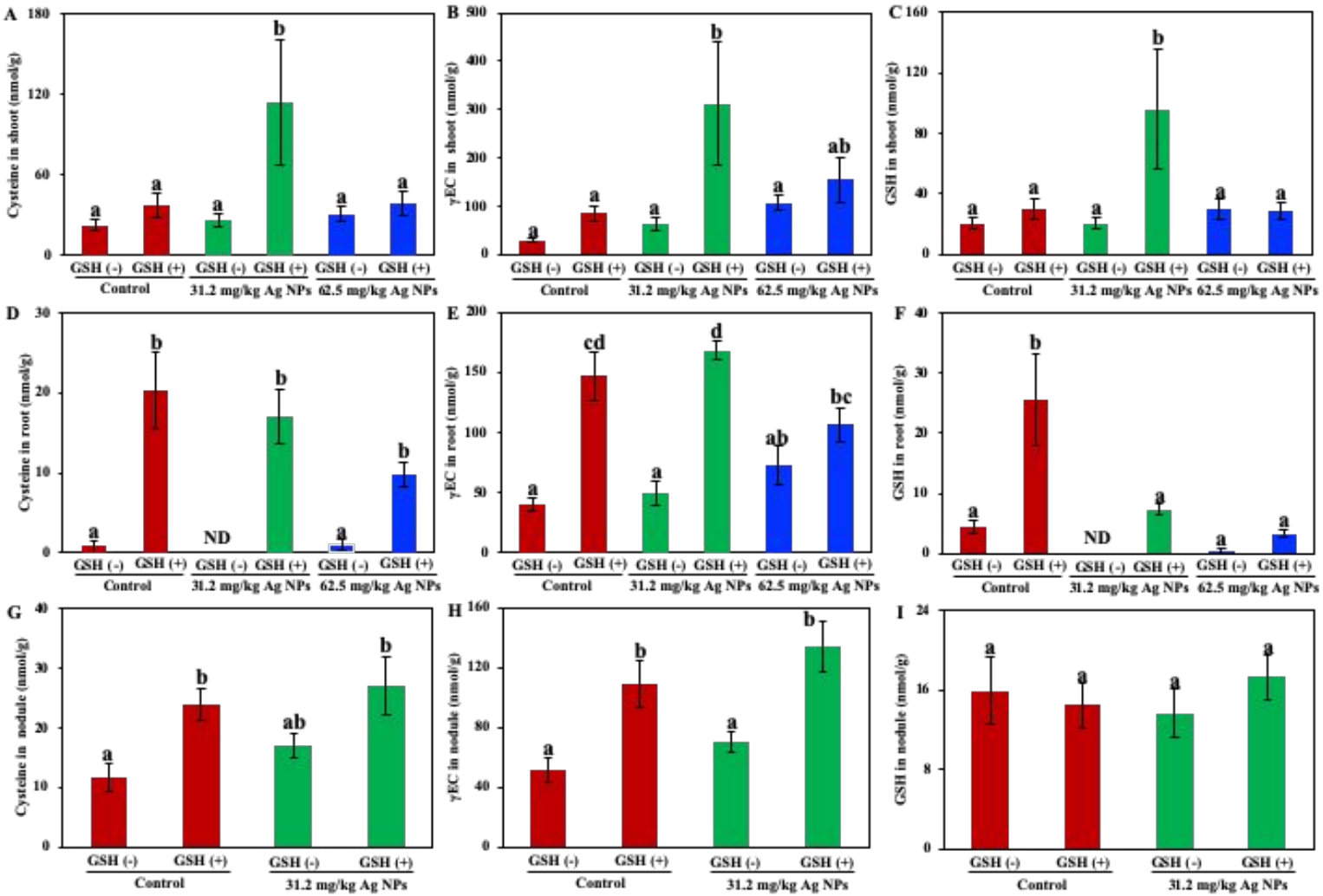

Figure 5. The content of thiol compounds involved in GSH biosynthesis pathway in Ag NPs treated soybean tissues w/ or w/o 0.8 mM GSH addition. Figure **A**, **D**, and **G** represents the cysteine content in soybean shoots, roots, and nodules, respectively; Figure **B**, **E**, and **H** represents the gamma-EC content in soybean shoots, roots, and nodules, respectively; Figure **C**, **F**, and **I** represent the GSH content in soybean shoots, roots, and nodules, respectively. Error bars correspond to standard error of mean. Values of each thiol compound in soybean tissues followed by different letters are significantly different at $p < 0.05$.

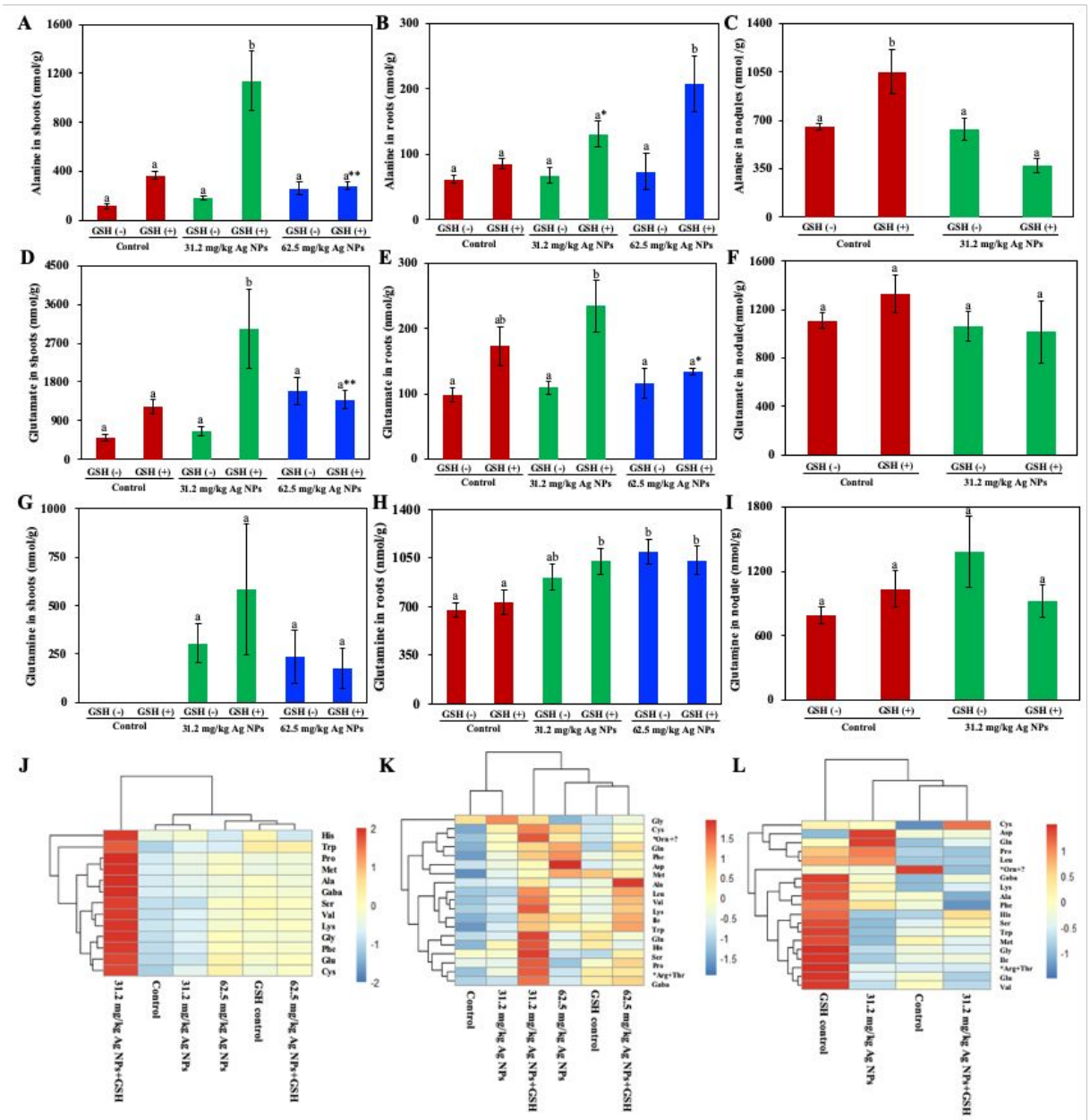

Figure 6. Amino acid profile in Ag NPs treated soybean tissues w/ or w/o the addition of 0.8 mM GSH. Figure **A–C** represents the content of alanine in soybean shoots, roots and nodules, respectively; Figure **D–F** is the content of glutamate in soybean shoots, roots and nodules, respectively; Figure **G–I** shows the content of glutamine in soybean shoots, roots and nodules, respectively; Figure **J–L** shows the heatmap of the amino acids profile of soybean shoots, roots and nodules, respectively. Error bars correspond to standard error of mean. Values of each amino acid followed by different letters are significantly different at $p < 0.05$. In Figure 6A and D, double asterisks indicate that the content of alanine and glutamate in the co-treatment of 62.5 mg/kg Ag NP and GSH is significantly higher as compared to the control at p=0.00267 and 0.00978, respectively, using a student t-test; in Figure 6B, single asterisk indicates the significant difference (p=0.0174) between the control and the 31.2 mg/kg Ag NP with the addition of GSH treatment by using a student t-test; in Figure 6H, single asterisk indicates the significant difference (p=0.0198) between the control and the 62.5 mg/kg Ag NP with the addition of GSH treatment using a student t-test.

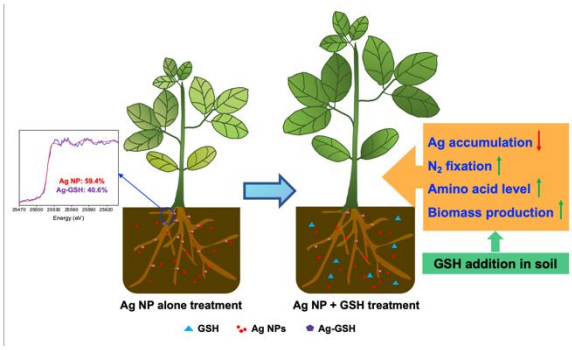
Ag NP: 59.4%
Ag-GSH: 40.6%
Energy (eV)
Ag accumulation
N2 fixation
Amino acid level
Biomass production
GSH addition in soil
Ag NP alone treatment
Ag NP + GSH treatment
GSH
Ag NPs
Ag-GSH

TOC art